Cryogenic thermal expansion and electrical conductivities of Mn_3CuN co-doped with Sb and Sn

Cite as: AIP Conference Proceedings **1435**, 393 (2012); https://doi.org/10.1063/1.4712121
Published Online: 12 June 2012

X. X. Chu, R. J. Huang, Z. X. Wu, Z. Chen, and L. F. Li

CRYOGENIC THERMAL EXPANSION AND ELECTRICAL CONDUCTIVITIES OF Mn_3CuN CO-DOPED WITH Sb AND Sn

X.X. Chu[1,2], R.J. Huang[1], Z.X. Wu[1,2], Z. Chen[1,2], Y. Zhou[1], and L.F. Li [1,*]

[1]Key Laboratory of Cryogenics, Technical Institute of Physics and Chemistry, Chinese Academy of Sciences, Beijing, 100190, P.R. China

[2]Graduate University of Chinese Academy of Sciences, Beijing, 100039, P.R. China

ABSTRACT

A series of Sb and Sn co-doped anti-perovskite Mn_3CuN materials were fabricated by mechanical ball milling followed by solid-state sintering. Their thermal expansion properties and electrical conductivities were investigated in the temperature range of 77-300 K. The results show that $Mn_3(Cu_xSb_{1-x})N$ (x=0.4, 0.5, 0.6, 0.7) exhibit negative thermal expansion (NTE) below 150 K, and the NTE temperature range shifts toward the lower temperature with the Sb increased. However, Sn doped in the $Mn_3(Cu_{0.5}Sb_xSn_{1-x})N$ can lead the NTE behavior shifts to room temperature and the NTE operation-temperature window (ΔT) becomes broader. The electrical conductivities of $Mn_3(Cu_{0.5}Sb_xSn_{1-x})N$ decrease with the temperature and Sb content increased.

KEYWORDS: Cryogenic, Negative thermal expansion, Electrical conductivity

INTRODUCTION

Control of thermal expansion is of vital importance in highly advanced industries. Even a small variation of the thermal expansion coefficient (CTE) degrades the performance of devices in many precise applications, or causes stresses and deformations

Advances in Cryogenic Engineering
AIP Conf. Proc. 1435, 393-400 (2012); doi: 10.1063/1.4712121

that will lead to reliability problems. For example, in cryogenic engineering, structural systems that undergo thermal shock when the temperature varies between room temperature and cryogenic temperature bear with little mismatch of CTE. It is well known that the majority of materials expand when the environmental temperature increases. Consequently, in general, it is difficult to control thermal expansion of a material in a pure form. As a particular type of functional materials, negative thermal expansion (NTE) materials [1,2], which contract upon heating, have significant practical value to control CTE of materials by forming composite materials.

Recently, giant NTE material over a wide temperature range has been demonstrated in anti-perovskite structured manganese nitrides Mn_3AN (A= Cu, Zn, Ga, etc) doped with Ge, Sn or Si [3-6]. This kind of semimetal NTE material attracts great attention as a candidate for practical thermal-expansion compensators for its great thermal expansion and electric properties. In Mn_3AN, the Mn_6N octahedron is a very stable basic chemical unit, whereas the other metal A is less bound to the N. Therefore, an important feather of Mn_3AN NTE materials is the magnitude of NTE and the working temperature are tunable with A site doping. Our previous works have reported that the NTE effect moves toward lower-temperature region and the operative temperature window becomes broader as well, with increasing Si doping content on Ge sites in $Mn_3Cu_{0.6}Si_xGe_{0.4-x}N$ [5,7]. We noticed that Sn is under Ge and Sb is behind Sn in the periodic table, consequently, how the Sn/Sb codoped in Cu site effect the NTE behavior interested us.

In this paper, Sn, Sb, and Sn/Sb doped Mn_3CuN polycrystalline materials were fabricated by a solid state method. Their thermal expansion properties and electrical conductivities were investigated in the temperature range of 77–300 K.

EXPERIMENTAL

Polycrystalline samples $Mn_3(Cu_xSn_{1-x})N$, $Mn_3(Cu_xSb_{1-x})N$ (x=0.4, 0.5, 0.6, 0.7) and $Mn_3(Cu_{0.5}Sb_xSn_{1-x})N$ (x=0.1, 0.2, 0.3, 0.4) were obtained by a conventional powder metallurgical method. The raw materials were the powders of Mn, Cu, Sb, and Sn with initial particles size of about 10 μm and the pure N_2 gas (99.999%). Firstly, the Mn_2N powder was synthesized by the solid-gas reaction of pure Mn particles and nitrogen gas in the furnace at 1023 K for 24 h. Then, the Cu, Sb, and Sn powders with masses calculated from the stoichiometric content were mixed with Mn_2N powder by ball milling under a purified argon atmosphere. The ball milling was conducted in a planetary ball mill with a ball-to-powder weight ratio of 10:1 at a rotation speed of 350 rpm for 12 h. Subsequently, the amorphous compound powders were pressed into pellets of 13 mm diameter and 2-4 mm thickness at room temperature. The preformed samples were sintered at 1123 K in a tube furnace under a purified argon atmosphere for 48 h.

The crystal structures and phase constitutions of the $Mn_3(Cu_{0.5}Sb_{0.5})N$ were characterized at room temperature by X-ray diffraction (XRD) analysis using a Rigaku D/max-RB diffractometer with Cu Kα radiation (λ = 0.154056 nm). Scanning Electron Microscope (SEM) photographs of $Mn_3(Cu_{0.5}Sb_{0.5})N$ was taken with a HITACHI S-4300 SEM. Meanwhile, energy dispersive X-ray spectroscopy (EDS) was used to examine the

elemental composition of this sample.

The linear thermal expansion of $Mn_3Cu_xX_{1-x}N$, $\Delta L/L_{(300\ K)}$, was measured by a strain gage attached on the sample surface over the temperature range of 77–300 K. This method was conventional and simple but requires a reference material with known thermal expansion. In our work, we used fused silica and the corresponding thermal expansion data for the calibration of the strain gage. The strain gauges in sample and quartz were connected to form a half-bridge circuit to measure the $\Delta R/R$, and the strain $\Delta L/L$ was collected by a computer. The electrical conductivity was measured using a standard four-probe method in the temperature range of 77–300 K.

RESULTS AND DISCUSSION

Structures

The indexed XRD patterns for $Mn_3(Cu_{0.5}Sb_{0.5})N$ compound at room temperature are given in figure 1. The XRD patterns show that this sample has a dominating phase with the Mn_3CuN-type structure (Pm3m). A few other diffraction peaks were found, which may come from a litter oxide in the surface. However, we can conclude that Sb-doping in Mn_3CuN does not change the anti-perovskite structure, so the Sb successfully introduced in Cu site. SEM image of $Mn_3(Cu_{0.5}Sb_{0.5})N$ compound are also shown in figure 2. Some small pores remain inside the sample, which may result from the release of excessive nitrogen in the process of sintering. From the EDS result in figure 3, it was determined that only manganese, copper, antimony and nitrogen were included in the crystallite.

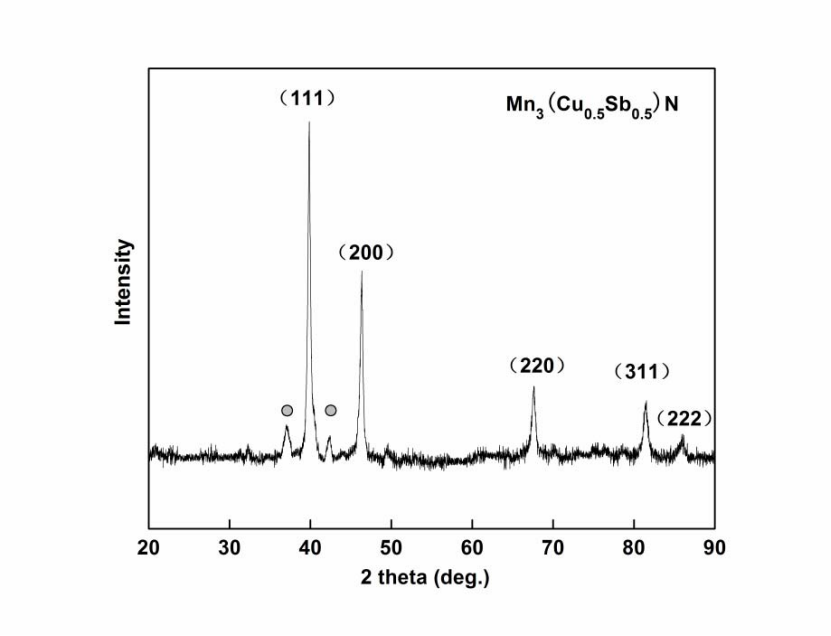

FIGURE 1. X-ray diffraction patterns of $Mn_3(Cu_{0.5}Sb_{0.5})N$ at room temperature.

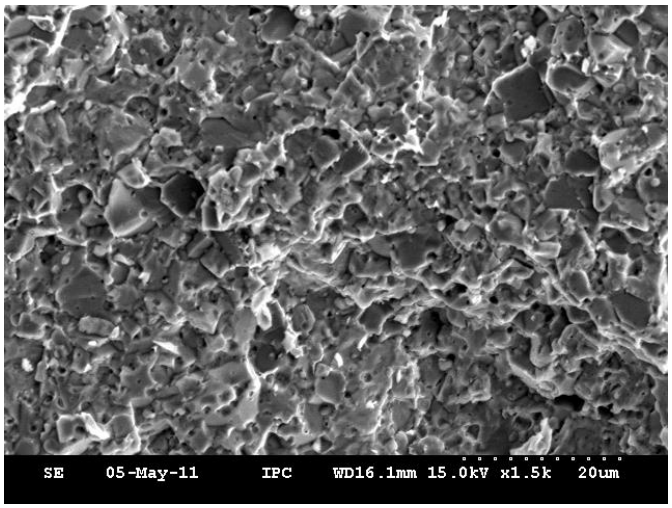

FIGURE 2. SEM image of $Mn_3(Cu_{0.5}Sb_{0.5})N$.

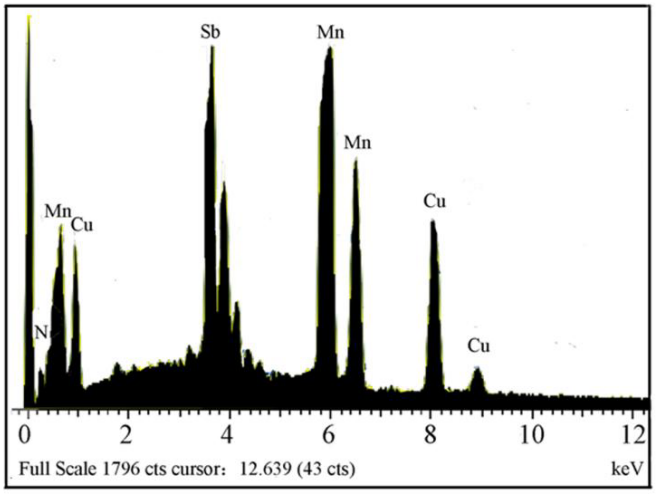

FIGURE 3. EDS data of $Mn_3(Cu_{0.5}Sb_{0.5})N$.

Negative Thermal Expansion Properties

Fig. 4(a) and Fig. 4(b) display the temperature dependence of the linear thermal expansions $\Delta L/L_{(300K)}$ for the $Mn_3(Cu_xSn_{1-x})N$ and $Mn_3(Cu_xSb_{1-x})N$ (x=0.4, 0.5, 0.6, 0.7). It is clear seen that except $Mn_3(Cu_{0.4}Sn_{0.6})N$, in other samples, there exists a temperature region in which the linear thermal expansion increases abruptly with decreasing temperature, i.e. NTE occurs. However, the operation-temperature window of NTE changes with varying Cu and Sn or Sb contents. In Fig. 4(a), we can see the sample $Mn_3(Cu_{0.7}Sn_{0.3})N$ displays NTE behavior at about 200 K. With the content of the partial replacement of Cu by Sn increased, the NTE behavior shifts to high temperature range. When x=0.5, the NTE operation-temperature window of $Mn_3(Cu_{0.5}Sn_{0.5})N$ is above room

temperature. This phenomenon is accordant with previous work [6], which reported the NTE temperature ranges moved to a higher temperature with the increasing Sn content in $Mn_3(Zn_xSn_{1-x})N$. However, in $Mn_3(Cu_xSb_{1-x})N$, the doping effect of Sb is just opposite to Sn. We can easily find that at high temperatures, the thermal expansion is almost independent of Sb content and the $\Delta L/L_{(300K)}$ is nearly linear in Fig. 4(b). The average CTE of $Mn_3(Cu_xSb_{1-x})N$ near room temperature is about 17×10^{-6}/K, that is comparable with Cu (16.5×10^{-6}/K). This tendency of CTE at high temperatures is nearly consistent with the Grüneisen formula, which suggests that the CTE is governed only by the anharmonic phonon contribution in this temperature range [4]. At low temperature, the NTE occurs and with the Sb content increased, the NTE windows shift toward cryogenic temperature. By the way, the NTE temperature ranges are very narrow. However, It is of particular interest that the variation of $\Delta L/L_{(300K)}$ data of $Mn_3(Cu_xSb_{1-x})N$ are small below the temperature of NTE temperature range. For example, the sample $Mn_3(Cu_{0.7}Sb_{0.3})N$ showed a low expansion of $|\alpha| < 0.5\times10^{-6}$/K in the temperature range of 130-77 K, which indicates that this material shows the Invar-like behavior in this temperature range. Unfortunately, we can't measure the CTE below liquid nitrogen temperature. We think even below 77 K, the Invar-like behavior will maintain in the material of some $Mn_3(Cu_xSb_{1-x})N$.

According to the above results, to obtain a cryogenic NTE behavior, the one way is increasing the ratio of Cu^{2+}/Sn^{4+} in the antiperovskite structure, the other is co-doped with Sn and Sb for Cu. The temperature dependence of $\Delta L/L_{(300K)}$ for the $Mn_3(Cu_{0.5}Sb_xSn_{1-x})N$ (x=0-0.5), which is Sn and Sb co-doped for Cu, is shown in Fig. 5. In this figure, we can easily find the NTE temperature ranges of Sn/Sb co-doped $Mn_3(Cu_{0.5}Sb_xSn_{1-x})N$ is between $Mn_3(Cu_{0.5}Sb_{0.5})N$ and $Mn_3(Cu_{0.5}Sn_{0.5})N$. With the Sb content increased, the NTE windows shift to low temperature. NTE temperature ranges can be tuned from 77 K to above room temperature by Sb/Sn codoped in $Mn_3(Cu_{0.5}Sb_xSn_{1-x})N$.

The NTE in manganese nitrides Mn_3AN originates from a large magnetovolume effect (MVC) which counteracts the normal thermal expansion, namely the magnetic ordering transition changes the magnetic atomic distance and induces the change of lattice volume. In our previous studies, the magnetic properties of the Mn_3CuN co-doped with Ge/Si were presented, in which the NTE behavior is accompanied by a paramagnetic to

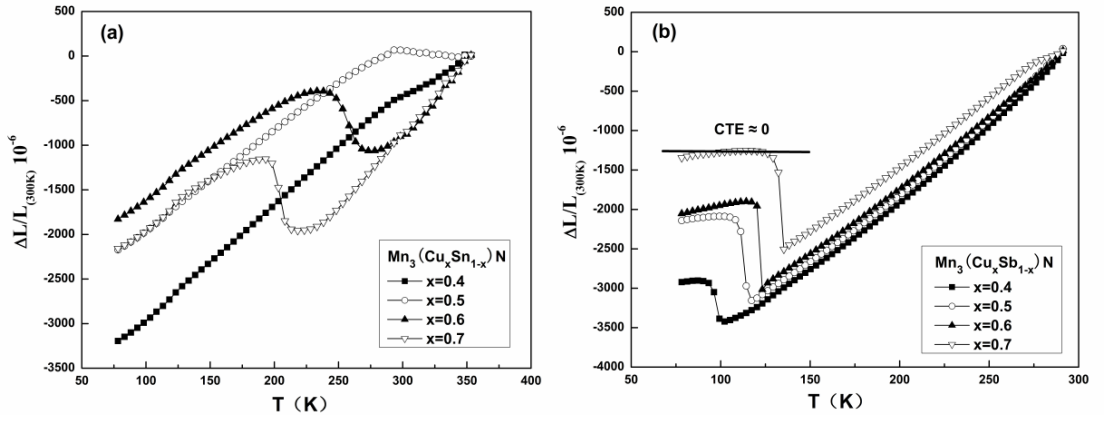

FIGURE 4. Linear thermal expansion coefficient of (a) $Mn_3(Cu_xSn_{1-x})N$ (x=0.4, 0.5, 0.6, 0.7) and (b) $Mn_3(Cu_xSb_{1-x})N$ (x=0.4, 0.5, 0.6, 0.7) in the temperature range of 77-350 K.

antiferromagnetic transition [5,8]. Some similar magnetic transitions will take place in the Mn_3CuN co-doped with Sn/Sb. However, we think the magnetic transition is not sufficient to introduce an obvious abrupt change of lattice constants. Thus, there may be other factors determining the change of the NTE temperature range. In Mn_3AN, the Mn atoms provide localized magnetic moments responsible for the magnetism, while the metal atoms on A sites provide the itinerant electrons at the Fermi level [9]. As a result, the magnetic transition temperature of Mn_3AN is scaled by electron concentration around element A. As we known, Sn and Sb are both in the fifth period in the periodic table, with Sb lying behind Sn. The electronic configuration of Sn is $4d^{10}5s^25p^2$, while for Sb the electronic shell is $4d^{10}5s^25p^3$. It can be seen that Sb has more free electrons than Sn in Mn_3AN at a given temperature. Meanwhile, the electronegativity of Sb (2.05) is larger than Sn (1.96), which means Sb has more ability to bound free electrons, resulting an increase of concentration and free energy of electron around site A. As a result, with the increasing of Sb element, the temperature range of NTE shifts to low temperature. Another possibility of Sb-doping make NTE temperature shift towards low temperature is the near nonmetal properties of Sb. This possibility reason needs further exploration in the future.

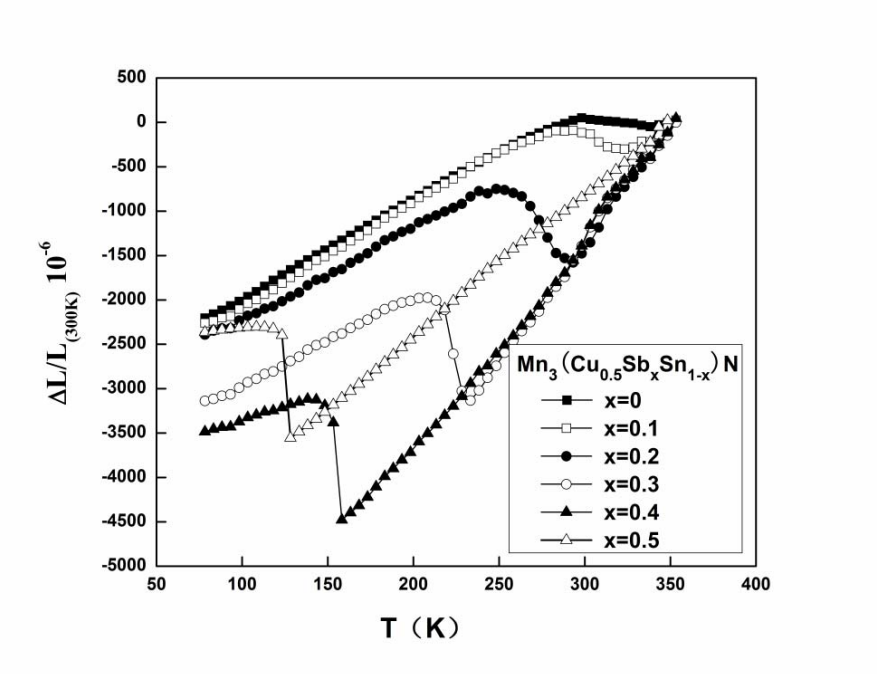

FIGURE 5. Linear thermal expansion coefficient of $Mn_3(Cu_{0.5}Sb_xSn_{1-x})N$ (x=0-0.5) in the temperature range of 77-350 K.

Electrical Conductivity

Most NTE materials, such as ZrW_2O_8 or $PbTiO_3$ type ceramics, are insulators. However, manganese nitride compound NTE material is semimetal and conductor. For

many applications, good electrical conductivity is also important as well as low thermal expansion behavior. For narrow-band-gap semimetals, both the carrier mobility and the carrier density, or the number of the carriers, are temperature-dependent. The temperature dependence of electrical conductivities of samples $Mn_3(Cu_{0.5}Sb_xSn_{1-x})N$ (x= 0.1, 0.3, 0.5) are shown in Fig. 6. The results show that with the increasing of Sb content, the electrical conductivities decrease obviously. This is because the antimony has a lower electrical conductivity compared with copper and tin. Furthermore, the electrical conductivities decrease monotonously with increasing temperature in the whole temperature range, which is a characteristic of metal. In previous report, Chi et al [10] discovered near-zero temperature coefficient of resistivity (TCR) in Mn_3CuN and Sun et al [11] reported low TCR behavior related the large lattice contraction in Mn_3NiN compound. However, in our studies, we find the NTE behaviors dependence of TCR (or electrical conductivity) is not obvious. Only in $Mn_3(Cu_{0.5}Sb_{0.5})N$ we find a little drop of electrical conductivity at about 110 K, which is correspond to its NTE temperature. In other samples, the electrical conductivities are almost independent of NTE behaviors. In Mn_3AN, the metal atoms on A sites offer itinerant electrons of the Fermi level. So the molecule structure and valence electron number of A atoms is a dominant factor for the electronic transport properties of Mn_3AN. We think the Sb and Sn codoped Mn_3CuN cause litter distortion in anti-perovskite structure. Since the mobility changes only in a mild way with the temperature, the temperature dependence of the electrical conductivity is dominated by the carrier density. Just like some semimetals, the number of carriers in $Mn_3(Cu_{0.5}Sb_xSn_{1-x})N$ can be an exponential-like function of 1/T [12]. Consequently, the temperature dependence of electrical conductivities of $Mn_3(Cu_{0.5}Sb_xSn_{1-x})N$ shows a semimetal behavior.

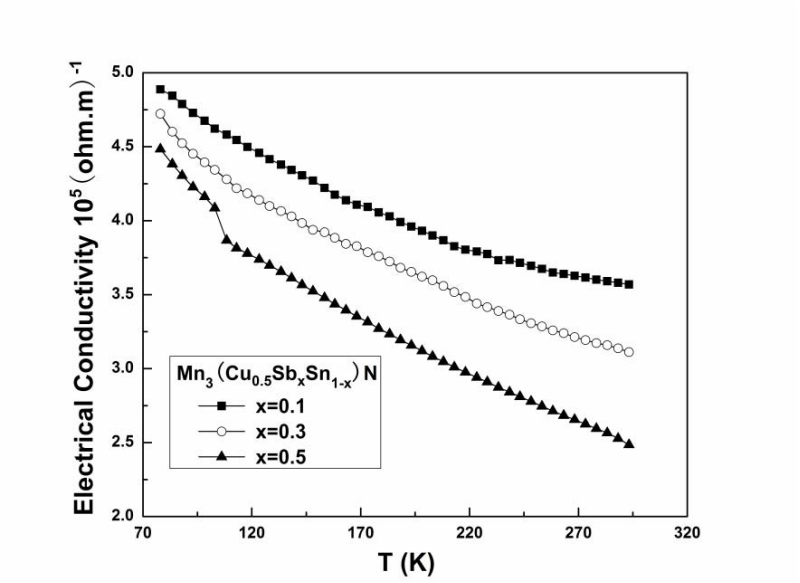

FIGURE 6. The electrical conductivities of $Mn_3(Cu_{0.5}Sb_xSn_{1-x})N$ (x=0.2, 0.3, 0.5) in the temperature range of 77-300 K.

CONCLUSION

In present work, $Mn_3(Cu_xSn_{1-x})N$, $Mn_3(Cu_xSb_{1-x})N$ (x=0.4, 0.5, 0.6, 0.7) and $Mn_3(Cu_{0.5}Sb_xSn_{1-x})N$ (x=0.1, 0.2, 0.3, 0.4) were synthesized by mechanical alloying followed by solid-state sintering. Their thermal expansion properties and electrical conductivities were investigated from 77 K to room temperature. The results show that the Sn-doping Mn_3CuN leads the operation-temperature window of NTE shifts toward high temperatures, while that of Sb-doping shifts toward cryogenic temperatures. Meanwhile, Sb-doping Mn_3CuN result in low CTE at cryogenic temperatures. $Mn_3(Cu_{0.7}Sb_{0.3})N$ shows a near zero CTE below its NTE temperature. The electrical conductivities exhibit a nearly linear decrease with increasing temperature. The NTE behaviors have litter affect on their electrical properties. Further studies are required for establishing the effects of Sn/Sb codoping and also for developing some negative or near zero thermal expansion materials, which may possibly be exploited to design the critical component in cryogenic engineering and aerospace areas.

ACKNOWLEDGEMENTS

This project is supported by the National Natural Science Foundation of China (Grant Nos. 51077123 and 10904153).

REFERENCES

[1] Miller, W, Smith, CW, Mackenzie, DS, Evans, KE. *Journal of Materials Science*; **44**, 5441-5451, (2009)

[2] Evans, JSO, Hu, Z, Jorgensen, JD, Argyriou, DN, Short, S, Sleight, AW. *Science*; **275**, 61-65, (1997)

[3] Takenaka, K, Takagi, H. *Applied Physics Letters*; **87**, 261902, (2005)

[4] Takenaka, K, Asano, K, Misawa, M, Takagi, H. *Applied Physics Letters*; **92**, 011927, (2008)

[5] Huang, RJ, Li, LF, Cai, FS, Xu, XD, Qian, LH. *Applied Physics Letters*; **93**, 081902, (2008)

[6] Sun, Y, Wang, C, Wen, YC, Chu, LH, Pan, H, Nie, M, Tang, MB. *J. Am. Ceram. Soc.*; **93**, 2178-2181, (2010)

[7] Huang, RJ, Wu, ZX, Chu, XX, Yang, HH, Chen, Z, Li, LF. *Solid State Sciences*; **12**, 1977-1980, (2010)

[8] Huang, RJ, Li, LF, Wu, ZX, Chu, XX, Xu, XD, Qian, LH. *Solid State Communications*; **150**, 1617-1620, (2010)

[9] Sun, Y, Wang, C, Wen, YC, Zhu, KG, Zhao, JT. *Applied Physics Letters*; **91**, 231913, (2007)

[10] Chi, EO, Kim, WS, Hur, NH. *Solid State Communications*; **120**, 307-310, (2001)

[11] Sun, Y, Wang, C, Chu, LH, Wen, YC, Nie, M, Liu, FS. *Scr. Mater.*; **62**, 686-689, (2010)

[12] Ji, AL, Li, CR, Cao, Z. *Applied Physics Letters*; **89**, 252120, (2006)